

## HUBBLE SPACE TELESCOPE OBSERVATIONS OF SUPERLUMINAL MOTION IN THE M87 JET

J. A. BIRETTA, W. B. SPARKS, AND F. MACCHETTO

Space Telescope Science Institute, 3700 San Martin Drive, Baltimore, MD 21218; biretta@stsci.edu

Received 1999 January 28; accepted 1999 March 8

### ABSTRACT

We present observations of the M87 jet made with the Faint Object Camera on board the *Hubble Space Telescope* at five epochs between 1994 and 1998. These observations reveal 10 superluminal features within the first 6" of the jet, with eight of these having apparent speeds in the range  $4c$ – $6c$ . Two additional features within the first arcsecond of the jet have subluminal speeds of  $0.63c$  and  $0.84c$ . The latter of these, named HST-1 East, appears to emit new superluminal features moving at  $6c$ , which subsequently fade with a half-intensity timescale of  $\sim 2$  yr. The fastest speeds we observe require a Lorentz factor  $\gamma \geq 6$  for the bulk flow and a jet orientation within  $19^\circ$  of the line of sight, in the context of the relativistic jet model. Finding such large  $\gamma$  in an FR I radio source like M87 strongly supports BL Lac/FR I unification models. These large speeds help to mitigate the particle lifetime problem posed by the optical emission, as well as the jet confinement problem.

*Subject headings:* galaxies: individual (M87) — galaxies: jets

### 1. INTRODUCTION

The existence of bulk relativistic motion in jets was first proposed by Shklovsky (1964) to explain the apparently one-sided optical jet in M87. Since that time, radio observations have provided evidence for superluminal motion, and hence relativistic flow, in the nuclei of many core-dominated radio sources (Porcas 1986). Unified models, in fact, predict that relativistic flow must be a common feature of radio galaxies if indeed radio galaxies are the parent population of quasars and BL Lac objects (Barthel 1989; Urry & Padovani 1995). The identification of relativistic motion in the parent radio galaxies is a crucial test of these models, but so far examples are few, and only modest speeds have been seen (Alef et al. 1994; Giovanini et al. 1998).

M87 (Virgo A, NGC 4486, 3C 274) is a giant elliptical galaxy near the center of the Virgo Cluster. Fanaroff & Riley (1974) classify it as a type I radio source based on its radio morphology, although its luminosity ( $P_{(178 \text{ MHz})} = 1.0 \times 10^{25} \text{ W m}^{-2}$ ) places it near the FR I/FR II division. It is one of the closest radio galaxies ( $D = 16 \text{ Mpc}$ ), and because of this proximity it is one of our best opportunities to study active galactic nuclei and nonthermal jet phenomena. In the nucleus, *Hubble Space Telescope* (*HST*) observations show the presence of a disk of ionized gas oriented normal to the jet (on the sky plane). Spectroscopic studies of this gas indicate the presence of a large mass,  $3 \times 10^9 M_\odot$ , within the central 3 pc of the galaxy, which provides strong evidence for a supermassive black hole (Harms et al. 1994; Macchetto et al. 1997).

The 20" long jet in M87 is a prominent source of radio, optical, and X-ray emission (Biretta, Stern, & Harris 1991; Biretta 1994). Detailed comparisons of radio and optical data show that, while there are remarkable similarities (Boksenberg et al. 1992), there are also significant systematic differences between the radio and optical jets: the optical emission is more concentrated in the knots and along the center line of the jet (Sparks, Biretta, & Macchetto 1996; Biretta et al. 1999a). These differences are further underscored by VLA and *HST* polarimetry, which show that the radio and optical emission must arise in somewhat separate regions with different magnetic field configurations (Perlman et al. 1999). Low-frequency VLA images show

that the jet continues to at least 10 kpc and appears to inflate two large cavities in the interstellar medium (ISM; Böhringer 1995; Owen, Eilek, & Kasim 1999).

Previous efforts to measure motions in the M87 jet have found typical speeds between  $0.5c$  and  $\sim c$  for the brightest regions (knots A and B, located 1–1.5 kpc from the nucleus), while superluminal motion at  $2c$ – $2.5c$  was found in two small features within knot D about 200 pc from the nucleus (Biretta, Zhou, & Owen 1995, hereafter BZO95). Somewhat mysteriously, VLBI observations of the nucleus have obtained very low velocities,  $\leq 0.03c$ , for four features within 5 pc of the core (Biretta & Junor 1995, hereafter BJ95; Junor & Biretta 1995).

Herein we present new results for the first 6" of the M87 jet, which are derived from *HST* observations ( $\sim 0.03$  resolution) at five epochs spanning 1994–1998. These results offer the first detection of optical superluminal motion and indicate characteristic apparent speeds of  $4c$ – $6c$ . These are the highest speeds yet seen in an FR I radio galaxy. For an assumed distance of 16 Mpc (Mould, Aaronson, & Huchra 1980; Tonry 1991; Whitmore et al. 1995), the linear scale is  $78 \text{ pc arcsec}^{-1}$ , and the motion at  $1 \text{ mas yr}^{-1}$  corresponds to an apparent velocity  $0.254c$ .

### 2. OBSERVATIONS AND ANALYSES

All observations were made with the *HST* Faint Object Camera (FOC) in the f/96 mode, which gives an image scale of  $0.01435 \text{ pixel}^{-1}$ , an effective resolution of  $\sim 35 \text{ mas}$ , and a field of view  $7'' \times 7''$ . Exposures were made in the F342W filter ( $\lambda = 342 \text{ nm}$ ), and the F4ND neutral density filter was used to avoid saturation in the nucleus (Table 1). Several measures were taken to optimize the geometric stability and repeatability of the images: The FOC was warmed up and exercised for  $\sim 10 \text{ hr}$  prior to each session; the jet was carefully placed on the same region of the detector; and finally, internal flats containing Reseau marks were taken throughout each session to monitor the geometric stability of the readout electronics (Nota et al. 1996).

Analysis of the images began with pipeline processing using the best geometric correction file (f371529ex.r5h). Each image was then rotated to place the jet on the  $X$ -axis using the header value of PA\_V3 and resampled to 3 times

TABLE 1  
OBSERVATION LOG

DATE	EXPOSURE TIME (s) FOR EACH FILTER	
	F342W	F342W + F4ND
1994 Aug 04 .....	1911	1679
1995 Jul 05 .....	2393	2066
1996 Jul 31 .....	2502	2226
1997 Jul 14 .....	2564	2227
1998 Jul 20 .....	2563	2227

smaller pixels. We then aligned the F342W + F4ND images from the different epochs using the nucleus as a reference point. Finally, for each epoch we aligned the F342W image with the F342W + F4ND image using the bright knot (knot L) approximately 0.16" from the nucleus as a reference point.

Position changes for jet features (Figs. 1–3) were measured using the two-dimensional cross-correlation technique described by BZ95. A small image region isolating each jet feature was selected, and this region was cross-correlated for a pair of adjacent epochs. The shift that maximized the cross-correlation was taken as the position change, and in all cases the peak cross-correlation was 0.95 or greater, indicating good signal-to-noise ratios. The total position change was then computed by summing the shifts between adjacent epochs. Uncertainties were also estimated with procedures similar to BZ95. Poisson noise was

added to each image whose variance was computed on a pixel-by-pixel basis according to the image intensity. The cross-correlation was then repeated, and a “perturbed” value of the position change was obtained. This procedure was repeated for 10 different noise models, and the uncertainty was estimated as the rms variation in the 10 perturbed values. The relative positions were then plotted (Fig. 1 insets), and proper motions were derived by linear least-squares fitting (Table 2). In all cases a straight line (constant velocity) is a reasonably good fit to the observed positions (reduced  $\chi^2 \leq 1.7$ ). Apparent velocities were computed from the proper motions assuming a distance of  $15.9 \pm 0.9$  Mpc (Tonry 1991; Whitmore et al. 1995). While this distance estimate is derived independently of  $H_0$ , it will still impose some uncertainty on the overall velocity scale; we have not included this uncertainty in Table 2.

Herein we primarily discuss the radial components of motion (i.e., parallel to the jet axis); for most features the transverse motion is negligible. A future paper will present details of the measurements and results for features beyond 6", which require mosaicking of several images.

### 3. RESULTS

We discuss each jet region (Fig. 1) in turn, beginning near the nucleus. Our images show a slow-moving, unresolved knot about 0.16" (12 pc) from the nucleus. It appears spatially coincident with knot L seen in 1.66 GHz VLBI images (Reid et al. 1989), and we have labeled it accordingly. The speed we observe,  $0.63c \pm 0.27c$ , is the slowest observed

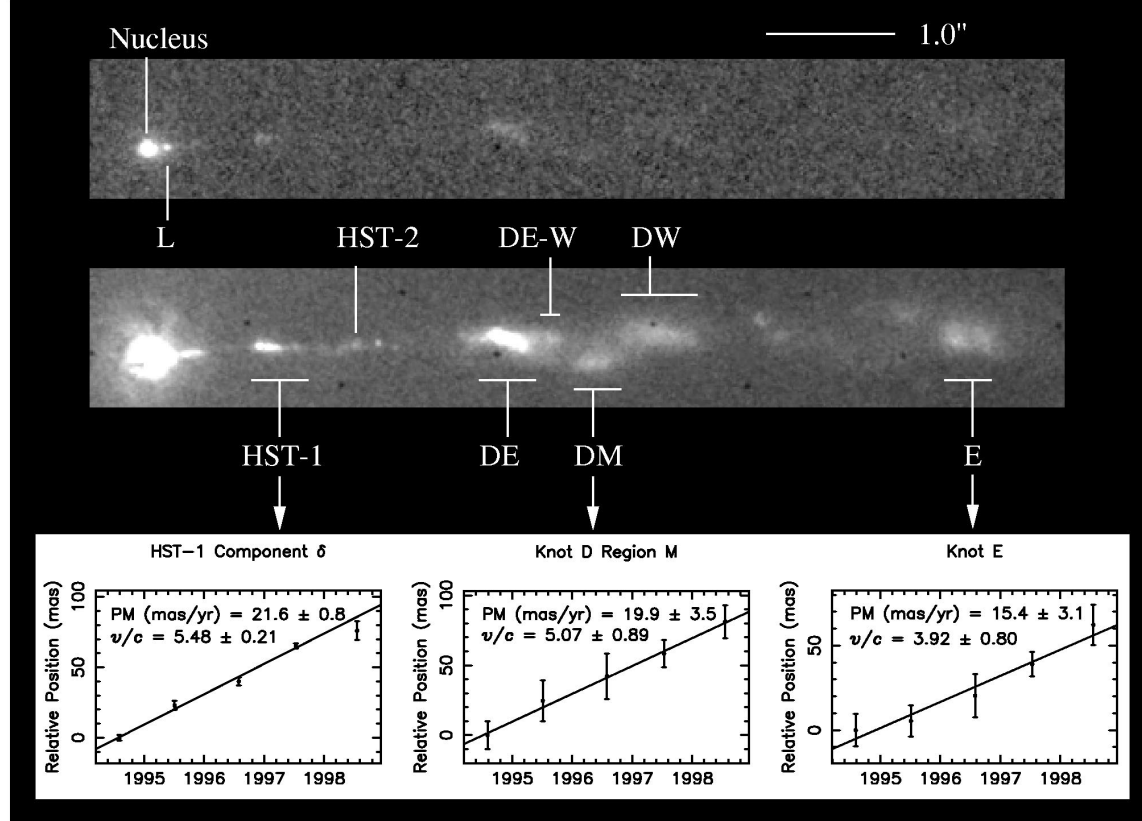


FIG. 1.—Locations of jet features discussed herein. The top panel is the 1994 image in the F342W + F4ND filters, and the bottom panel is F342W alone. Dark spots in the lower panel are Reseau marks on the photocathode. The image has been rotated from its normal appearance on the sky in such a way that the X-axis is along P.A. 290°. Inset plots show relative position vs. epoch for three representative features; fitted proper motions (PMs) and derived speeds in units of  $v/c$  are indicated.

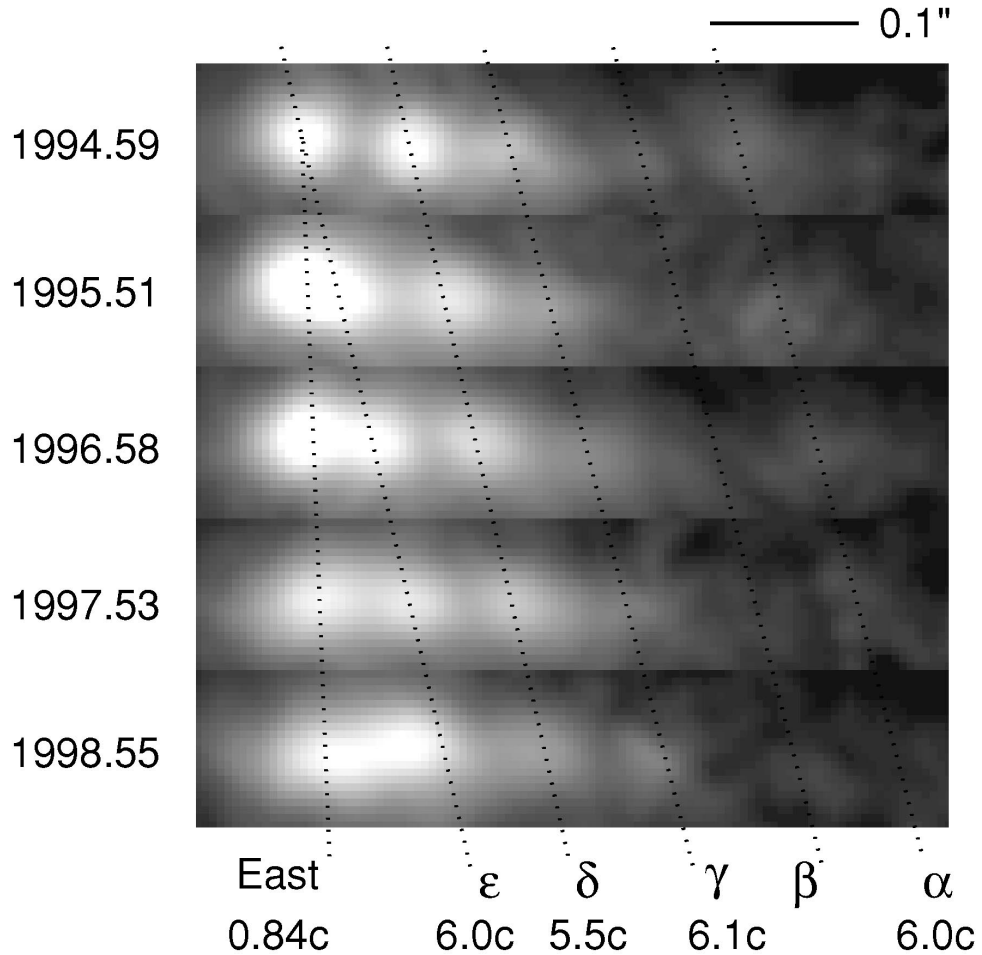


FIG. 2.—Sequence of F342W images showing evolution of HST-1 region between 1994 and 1998. The dotted lines attempt to identify and track features between epochs and are labeled with feature names and speeds derived herein.

herein and is consistent with the lack of motion for the coincident VLBI feature (BJ95). While the low speed seems surprising given results farther below, we note that the bright VLBI features near the core also have very low speeds ( $<0.03c$ ; BJ95; Junor & Biretta 1995).

The region we have named HST-1 appears as a linear chain of compact components extending along the jet and located  $\sim 80$  pc from the nucleus. HST-1 has a fascinating evolution, showing both slow and fast features as well as the birth of new components and the fading of older ones. The

TABLE 2  
PROPER MOTIONS OF JET FEATURES

Feature	Distance from Nucleus <sup>a</sup> (arcsec)	Feature Size <sup>b</sup> (arcsec)	Proper Motion <sup>c</sup> (mas yr <sup>-1</sup> )	$v/c$ <sup>d</sup>
L.....	0.16	0.06	$2.49 \pm 1.05$	$0.63 \pm 0.27$
HST-1 East.....	0.87	$\leq 0.05$	$3.31 \pm 0.43$	$0.84 \pm 0.11$
HST-1 $\epsilon$ .....	0.87	$\leq 0.05$	$23.6 \pm 1.9$	$6.00 \pm 0.48$
HST-1 $\delta$ .....	0.94	$\leq 0.05$	$21.6 \pm 0.8$	$5.48 \pm 0.21$
HST-1 $\gamma$ .....	0.99	$\leq 0.05$	$24.2 \pm 2.3$	$6.14 \pm 0.58$
HST-1 $\alpha$ .....	1.16	$\leq 0.1$	$23.7 \pm 4.1$	$6.02 \pm 1.05$
HST-2.....	1.61	0.1	$20.1 \pm 2.6$	$5.11 \pm 0.66$
DE .....	2.75	0.1–0.4	$11.8 \pm 1.1$	$2.99 \pm 0.28$
DE-W .....	3.1	0.2	$17.9 \pm 2.7$	$4.54 \pm 0.69$
DM .....	3.4	0.3	$19.9 \pm 3.5$	$5.07 \pm 0.89$
DW .....	4.0	0.6	$10.5 \pm 3.7$	$2.66 \pm 0.94$
E.....	6.3	0.4	$15.4 \pm 3.2$	$3.92 \pm 0.80$

<sup>a</sup> Approximate distance from nucleus for epoch 1994.

<sup>b</sup> Approximate feature size in direction parallel to jet axis. Feature DE contains multiple components with a range of scale sizes.

<sup>c</sup> Component of motion parallel to jet axis. Positive values indicate motion away from the nucleus and toward P.A. 290°.5.

<sup>d</sup> Apparent velocity in units of  $c$ , the velocity of light, for an assumed distance of 16 Mpc.

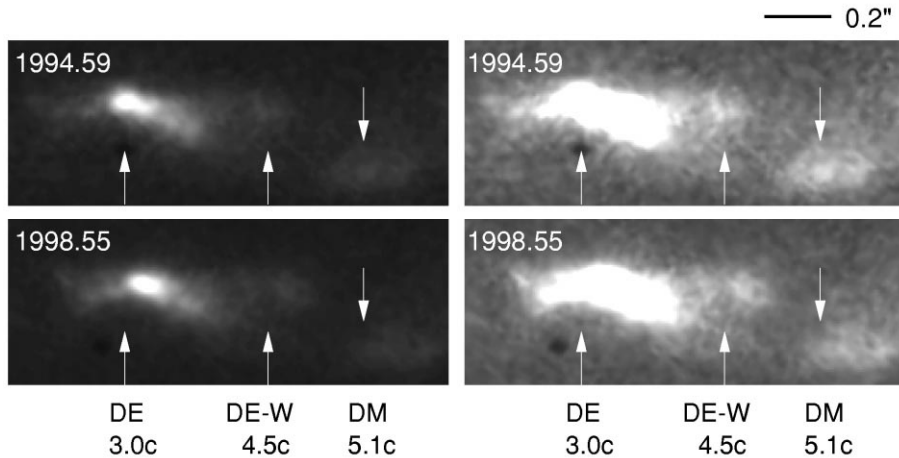


FIG. 3.—Pair of F342W images from 1994 and 1998 illustrating motions in knot D. The arrows indicate features DE, DE-W, and DM and also serve as fiducial points to judge motions. Derived speeds are indicated. Left panels show bright features, and right panels show faint ones.

easternmost component of the chain (HST-1 East; Fig. 2) moves outward relatively slowly at  $0.84c \pm 0.11c$  and appears to be the origin of at least three western components moving with speeds between  $5.5c$  and  $6c$ . We label these, from east to west, HST-1 $\delta$ , HST-1 $\gamma$ , and HST-1 $\alpha$ . A weaker feature, HST-1 $\beta$ , is seen in 1994, but it is difficult to discern at later epochs. Beginning in 1995, HST-1 East appears to eject a new component (HST-1 $\epsilon$ ) with speed similar to the other western components of HST-1. A second, weaker ejection event may have occurred in 1998. (We have omitted the 1998 data from the linear fits for HST-1 East and  $\epsilon$ , since the structure becomes complex.) The fast western components fade with a half-intensity timescale of about 2 yr, while the brightness of HST-1 East varies by  $\pm 20\%$ . Figure 2 suggests periodic ejection from HST-1 East (period  $\sim 3$  yr) with newly born components possibly having some differences in brightness.

The individual features appear unresolved, with the possible exception of HST-1 $\alpha$ . An adjacent feature that we have named HST-2 is slightly resolved and appears to move outward at  $5.11c \pm 0.66c$ , which is comparable to features in HST-1. In the radio band, the region comprising HST-1

and HST-2 appears as a relatively smooth, narrow, continuous knot extending for  $1''$  along the jet (knot H of Zhou 1998); it displays variability and structural changes, but motions are poorly determined.

Within knot D we have measured speeds for four features, and they range from  $2.7c \pm 0.9c$  to  $5.1c \pm 0.9c$  (Fig. 3). The fastest speeds in knot D are for regions DE-W and DM, and they are consistent with the fastest speeds seen elsewhere in the jet. The upstream feature, DE, is significantly slower, with  $2.99c \pm 0.28c$  versus  $5.48c \pm 0.21c$  as seen in HST-1 $\delta$ .

Knot E is the feature farthest from the nucleus for which we have attempted to measure an optical speed. With a speed of  $3.92c \pm 0.80c$ , it is comparable to many other features, although marginally slower than the fastest speeds of  $5.5c$ – $6c$  in HST-1. The optical feature we measure in knot E is located near the jet axis, and it appears to be only one component of a much larger, complex region seen in the radio images.

Nearly all of the features move radially outward from the nucleus (within the uncertainties). The only exception is DE, which shows a slight component of motion normal to the jet axis toward the south at  $\sim 0.7c \pm 0.3c$ . None of the individual features show appreciable evidence for acceleration or deceleration. (Details are deferred to a later paper [Biretta et al. 1999b].)

Proper motions have previously been measured in the M87 jet using VLA radio observations with  $0''.15$  resolution (BZO95). Most of the radio features studied by BZO95 were at larger distances from the nucleus than those here and show speeds ranging from  $\sim -0.2c$  to  $1.2c$  (Fig. 4). Three features in knot D, however, are common to both our optical measurements and BZO95's. For two of the features, DM and DW, the radio and optical speeds are roughly similar. The third feature shows a large difference; DE was found to be stationary in the radio data ( $-0.2c \pm 0.1c$ ), but here it is superluminal with speed  $3.0c \pm 0.3c$ . This is due in part to DE being poorly resolved in the radio, together with structural differences and a tendency for the radio emission to be more extended (Sparks et al. 1996; Biretta et al. 1999a).

#### 4. SUMMARY AND DISCUSSION

We have measured proper motions for 12 features within the first  $6''$  (500 pc) of the M87 jet. Of these, 10 appear to be

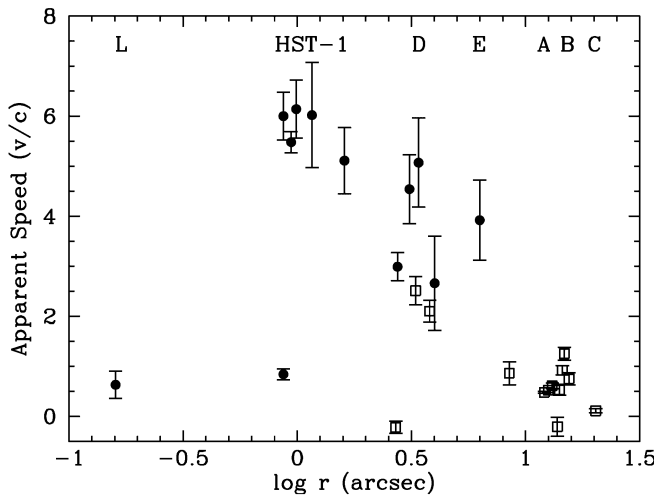


FIG. 4.—Plot showing measured apparent speed vs. distance from the nucleus ( $r$ ). Data from this paper are plotted as filled circles, and BZO95 radio data are plotted as open squares. Positions of knots are labeled across the top.

superluminal, with eight having apparent speeds in the range  $4c$ – $6c$ . The two subluminal features, knot L and HST-1 East, have speeds of  $0.63c \pm 0.27c$  and  $0.84c \pm 0.11c$ , respectively, and coincidentally are the two features nearest the nucleus (Fig. 4).

The most natural explanation for the observed superluminal speeds is that they are due to bulk relativistic flow in the context of the relativistic jet model (Blandford & Königl 1979a). The predominance of speeds in the range  $4c$ – $6c$  (the upper envelope of points in Fig. 4) suggests that these are closely linked to an underlying bulk flow. Several regions have much lower speeds, but we attribute this to obstructions or standing shocks within the jet (e.g., Blandford & Königl 1979b). Alternative models that invoke phase effects to produce superluminal motion (e.g., Dent 1972; Hardee & Norman 1989; Fraix-Burnet 1990) seem unlikely to work in M87. The consistency of the large speeds in different regions of the M87 jet, as well as the lack of large negative speeds, argues against phase effects as the source of motion.

The observed speeds provide strong constraints on the bulk flow speed and line-of-sight angle for the jet. The strongest constraints result from the largest apparent speeds, and hence we will use the value  $\sim 6c$  seen for several regions in HST-1. We also assume that the flow velocity is directed parallel to the jet axis. Hence the relativistic jet model requires a bulk flow with Lorentz factor  $\gamma \geq 6$  and a jet orientation within  $\theta \leq 19^\circ$  of the line of sight. Table 3 gives various allowed combinations of  $\gamma$  and  $\theta$ . There we also give implied parameters, including the jet Doppler shift factor  $\delta = 1/[\gamma(1 - \beta \cos \theta)]$ , the jet brightness boost  $B = \delta^3$ , and the jet/counterjet brightness ratio  $R = [(1 + \beta \cos \theta)/(1 - \beta \cos \theta)]^3$ , that assume a spectrum of the form  $S_\nu \propto \nu^{-1}$ . We have omitted solutions with small  $\theta$  (e.g.,  $\gamma \geq 8$  also has solutions with  $\theta < 3^\circ$ ), since they are geometrically improbable.

Solutions that place the jet farthest from the line of sight, and that are therefore favored in a probabilistic sense, require larger Lorentz factors (e.g.,  $\theta \sim 18^\circ$  implies  $\gamma \sim 12$ ). These solutions have Doppler factors near unity and only modest brightness boosts, and they may offer an explanation for the apparent lack of superluminal motion in M87 on parsec scales (BJ95). For this  $(\gamma, \theta)$  we lie just outside the beaming cone of the fast jet material. Hence the visible parsec-scale features in M87 may reside in slower ( $\gamma \sim 2$ ) layers near the jet surface (Laing 1994) or possibly represent regions where obstructions or stationary shocks perturb the streamlines, thereby broadening the effective beaming cone. The core-dominated radio sources (Pورcas 1986) may well be intrinsically similar to M87 but oriented at  $\theta \sim 5^\circ$ , where strongly beamed emission and fast superluminal features dominate the observed brightness. (Tsvetanov et al. 1998

has also proposed misdirection of the beaming cone based on variability of the nucleus.)

We note that all solutions imply very large jet-to-counterjet brightness ratios, owing to strong dimming of the receding counterjet. Ratios are  $4 \times 10^4$  or larger, which are entirely consistent with the lack of a detected counterjet. For example, Stiavelli, Moller, & Zeilinger (1992) give  $R > 450$  in the optical, and Biretta, Owen, & Cornwell (1989) find  $R > 150$  in the radio band.

Placing the jet within  $20^\circ$  of the line of sight presents several challenges. The presence of a sharp edge in knot A, if it represents a shock normal to the jet axis, implies  $\beta \sim \cos \theta \sim 0.43$  because of relativistic aberration (using the observed speed of knot A; BZO95), which disallows the parameters in Table 3. This can be resolved if knot A, instead, represents a highly oblique shock. In the model of Bicknell & Begelman (1997),  $(\theta, \gamma) \sim (18^\circ, 12)$  would require an obliquity of  $\psi_{\text{jet}} \sim 50^\circ$  in their notation, with very little cold matter content in the jet (their  $R_j \ll 1$ ). (Evidence for mild deceleration of the upper envelope in Fig. 4. is also consistent with knot D being a weak shock, as they suggest.) A second concern is the orientation of the nuclear gas disk, which Ford et al. (1994) suggest has its axis inclined  $\sim 42^\circ$  to the line of sight. This would place the jet and disk axes  $\sim 20^\circ$  apart, but a similar misalignment is already seen on the sky plane for M87 as well as in other radio galaxies (Ford et al. 1999). Another possibility is that the jet axis and velocity vectors are not aligned (as we assume). This might result, for example, if the features moved on helical tracks within the jet. At first glance, the predominance of radial motions argues against this, but detailed modeling is probably needed.

Our results strongly confirm “unified models,” which propose that FR I radio galaxies like M87 are the parent population of BL Lac objects (Browne 1983). Urry, Padovani, & Stickel (1991) predict that FR I radio galaxies should have jets with bulk flow speeds in the range from  $\gamma \sim 5$  to  $\sim 35$ , with most near  $\gamma \sim 7$ , which is in good agreement with speeds  $\gamma \geq 6$  implied by our observed  $6c$ . Furthermore, they derive a critical angle  $\theta_{\text{crit}} \sim 10^\circ$  for the FR I/BL Lac division, which is consistent with the angle  $\theta \sim 10^\circ$ – $19^\circ$  we favor for M87.

These speeds of  $6c$  are in fact the fastest yet seen for an FR I radio source. Superluminal motion has been recently reported in only one other FR I, 1144+35, with speed  $1.7c$  based on VLBI observations (Giovannini et al. 1998). Subluminal motion has been seen in the radio cores of several FR I galaxies including Cen A (Tingay et al. 1998), 3C 338 (Giovannini et al. 1994), and, of course, M87 itself (BJ95).

The “particle lifetime” problem and the confinement of jets are two key problems remaining in our understanding of these objects. The lifetime problem may be summarized

TABLE 3  
POSSIBLE SOLUTIONS FOR APPARENT SPEED  $\beta_{\text{app}} = 6^a$

Bulk Lorentz Factor ( $\gamma$ )	Line-of-Sight Angle ( $\theta$ ) (deg)	Jet Doppler Factor ( $\delta$ )	Jet Brightness Boost ( $B$ )	Jet/Counterjet Brightness Ratio ( $R$ )
6 .....	10	5.7	190	$3 \times 10^5$
8 .....	16	2.7	20	$8 \times 10^4$
10 .....	17	2.1	9	$7 \times 10^4$
12 .....	18	1.6	4	$5 \times 10^4$
40 .....	19	0.5	0.1	$4 \times 10^4$

<sup>a</sup> We have omitted solutions with  $\theta < 10^\circ$ .

by noting that optically emitting electrons in knot A of M87 have a lifetime against energy loss through synchrotron radiation of only  $\sim 300$  yr, yet this knot is at least 1 kpc from the nucleus. Particle acceleration is sometimes invoked as the solution, but detailed modeling has difficulty producing the correct spectra (see Biretta et al. 1991; Biretta 1994). Also, comparison of estimated pressures in the knots show that they significantly exceed those of the external medium, leading to problems explaining their apparent confinement (Owen, Hardee, & Cornwell 1989). Heinz & Begelman (1997) have explored relativistic beaming in M87 and its implications for magnetic field strength, particle lifetimes, and total pressure. They find that the lifetime and

confinement problems can be mitigated by relativistic effects together with subequipartition fields and suggest  $\gamma > 3$  and  $\theta \leq 25^\circ$  for the jet, which is consistent with our results. In particular,  $\gamma \sim 8$  and  $\theta \sim 16^\circ$  (consistent with observed apparent speeds  $\sim 6c$ ) imply fields about half the equipartition strength and pressures very close to those estimated for the ISM (White & Sarazin 1988).

We thank R. Jedrzejewski, T. Ellis, H. Hart, and H. Forrest for assistance during the real-time observations, and E. Perlman, C. Impey, and M. Livio for helpful comments. This work was supported by NASA grants GO-05941 and GO-07274.

## REFERENCES

Alef, W., Preuss, E., Kellermann, K. I., Wu, S. Y., & Qiu, Y. H. 1994, in *Compact Extragalactic Radio Sources*, ed. J. A. Zensus & K. I. Kellermann (Green Bank, MD: NRAO), 55

Barthel, P. D. 1989, *ApJ*, 336, 606

Bicknell, G. V., & Begelman, M. C. 1996, *ApJ*, 467, 597

Biretta, J. A. 1994, in *Astrophysical Jets*, ed. D. Burgarella, M. Livio, & C. P. O'Dea (Cambridge: Cambridge Univ. Press), 263

Biretta, J. A., & Junor, W. 1995, *Proc. Natl. Acad. Sci.*, 92, 11364 (BJ95)

Biretta, J. A., Owen, F. N., & Cornwell, T. J. 1989, *ApJ*, 342, 128

Biretta, J. A., Stern, C. P., & Harris, D. E. 1991, *AJ*, 101, 1632

Biretta, J. A., Zhou, F., & Owen, F. N. 1995, *ApJ*, 447, 582 (BZO95)

Biretta, J. A., et al. 1999a, in *The Radio Galaxy M87*, ed. H.-J. Röser & K. Meisenheimer (Heidelberg: Springer), in press

—. 1999b, in preparation

Blandford, R. D., & Königl, A. 1979a, *ApJ*, 232, 34

—. 1979b, *ApJ*, 20, L15

Böhringer, H., Nulsen, P. E. J., Braun, R., & Fabian, A. C. 1995, *MNRAS*, 274, L67

Boksenberg, A., et al. 1992, *A&A*, 261, 393

Browne, I. W. A. 1983, *MNRAS*, 204, 23P

Dent, W. A. 1972, *ApJ*, 175, L55

Fanaroff, B. L., & Riley, J. M. 1974, *MNRAS*, 167, 31P

Ford, H. C., et al. 1994, *ApJ*, 435, L27

—. 1999, in *The Radio Galaxy M87*, ed. H.-J. Röser & K. Meisenheimer (Heidelberg: Springer), in press

Fraix-Burnet, D. 1990, *A&A*, 227, 1

Giovannini, G., et al. 1994, in *Compact Extragalactic Radio Sources*, ed. J. A. Zensus & K. I. Kellermann (Green Bank, MD: NRAO), 61

—. 1998, in *IAU Colloq. 164, Radio Emission from Galactic and Extragalactic Compact Sources*, ed. J. A. Zensus, G. B. Taylor, & J. M. Wrobel (San Francisco: ASP), 85

Hardee, P. E., & Norman, M. L. 1989, *ApJ*, 342, 680

Harms, R. J., et al. 1994, *ApJ*, 435, L35

Heinz, S., & Begelman, M. C. 1997, *ApJ*, 490, 653

Junor, W., & Biretta, J. A. 1995, *AJ*, 109, 500

Laing, R. 1994, in *Astrophysical Jets*, ed. D. Burgarella, M. Livio, & C. P. O'Dea (Cambridge: Cambridge Univ. Press), 95

Macchetto, F. D., Marconi, A., Axon, D. J., Capetti, A., Sparks, W., & Crane, P. 1997, *ApJ*, 489, 579

Mould, J., Aaronson, M., & Huchra, J. 1980, *ApJ*, 238, 458

Nota, A., et al. 1996, in *FOC Instrument Handbook*, version 7.0 (Baltimore: STScI)

Owen, F. N., Eilek, J., & Kasim, N. 1999, in preparation

Owen, F. N., Hardee, P. E., & Cornwell, T. J. 1989, *ApJ*, 340, 698

Perlman, E., Biretta, J., Zhou, F., Sparks, W., & Macchetto, F. 1999, *AJ*, 117, 2185

Porcas, R. W. 1986, in *Superluminal Radio Sources*, ed. J. A. Zensus & T. J. Pearson (Cambridge: Cambridge Univ. Press), 12

Reid, M. J., Biretta, J. A., Junor, W., Spencer, R., Muxlow, T. 1989, *ApJ*, 336, 125

Shklovsky, I. S. 1964, *Soviet Astron.*, 7, 748

Sparks, W., Biretta, J., & Macchetto, F. 1996, *ApJ*, 473, 254

Stiavelli, M., Möller, P., & Zeilinger, W. W. 1992, *Nature*, 354, 132

Tingay, S. J., et al. 1998, in *IAU Colloq. 164, Radio Emission from Galactic and Extragalactic Compact Sources*, ed. J. A. Zensus, G. B. Taylor, & J. M. Wrobel (San Francisco: ASP), 87

Tonry, J. L. 1991, *ApJ*, 373, L1

Tsvetanov, Z. I., et al. 1998, *ApJ*, 493, L83

Urry, C. M., & Padovani, P. 1995, *PASP*, 107, 803

Urry, C. M., Padovani, P., & Stickel, M. 1991, *ApJ*, 382, 501

White, R. E., & Sarazin, C. L. 1988, *ApJ*, 335, 688

Whitmore, B. C., Sparks, W. B., Lucas, R. A., Macchetto, D. F., & Biretta, J. A. 1995, *ApJ*, 454, L73

Zhou, F. 1998, Ph.D. thesis, New Mexico Inst. Mining Tech.